

## Electromagnetic Signals and Backgrounds in Heavy-Ion Collisions

Sourendu Gupta  
HLRZ, c/o KFA Jülich, D-52425 Jülich, Germany

Aspects of the dilepton spectrum in heavy-ion collisions are discussed, with special emphasis on using lattice computations to guide the phenomenology of finite temperature hadronic matter. The background rates for continuum dileptons expected in forthcoming experiments are summarised. Properly augmented by data from ongoing measurements at HERA, these rates will serve as a calibrating background for QGP searches. Recent results on the temperature dependence of the hadronic spectrum obtained in lattice computations below the deconfinement transition are summarised. Light vector meson masses are strongly temperature dependent. Accurate measurements of a resolved  $\rho$ -peak in dimuon spectra in present experiments are thus of fundamental importance.

*Invited talk at the Quark Matter '93 Conference, Borlänge, Sweden, June 1993*

# Electromagnetic Signals and Backgrounds in Heavy-Ion Collisions

Sourendu Gupta <sup>a</sup>

<sup>a</sup>HLRZ, c/o KFA Jülich, D-5170 Jülich, Germany

Aspects of the dilepton spectrum in heavy-ion collisions are discussed, with special emphasis on using lattice computations to guide the phenomenology of finite temperature hadronic matter. The background rates for continuum dileptons expected in forthcoming experiments are summarised. Properly augmented by data from ongoing measurements at HERA, these rates will serve as a calibrating background for QGP searches. Recent results on the temperature dependence of the hadronic spectrum obtained in lattice computations below the deconfinement transition are summarised. Light vector meson masses are strongly temperature dependent. Accurate measurements of a resolved  $\rho$ -peak in dimuon spectra in present experiments are thus of fundamental importance.

## 1. Introduction

Electromagnetic probes of the quark gluon plasma have been surveyed extensively in the last few years. I will not repeat the material covered by these excellent reviews [1]. Since there has not been much development in the theory of photon signals since the last Quark Matter meeting, therefore, in the rest of this talk I will concentrate on dilepton signals and backgrounds.

Recall that mass spectra for opposite sign dileptons form a continuum with conspicuous resonances sitting over it. The cross section is very closely related to a theorist's favourite quantity—the spectral density of a vector correlation function. All observed resonances correspond to flavour singlet vector mesons. With sufficient mass resolution in the spectra the fate of each such meson can be seen in the dense and, possibly, thermalised hot matter formed as a result of heavy ion collisions. The ease with which individual resonances can be isolated and studied by well-designed experiments makes the dilepton signal a tool which is neglected only by the most foolhardy physicist. The continuum itself may be interesting for various reasons, many of which have been reviewed before.

I shall spend most of my allotted pages on scenarios which are built for matter in, or not far from, thermal equilibrium. The main reason for this emphasis is the ease with which theorists can do these computations; but, as reported in this meeting [2,3], there are model computations now which indicate a fairly short thermalisation times in heavy-ion collisions. Nevertheless, it is necessary to keep in mind that the dense systems formed may spend a significant fraction of their lifetimes trying to come to a state of equilibrium. If they succeed, they will be doing much better than most people.

Uptil now very little work has been done with non-equilibrium scenarios. It should be mentioned that Shuryak's two-step thermalisation model [4] is an attempt at constructing a toy model of non-equilibrium phenomena. Other such attempts are hydrodynamical shock waves and burning walls [5], swiss-cheese instabilities [6], *etc.* All these dynamical

modes can be married to standard dilepton production processes, thereby yielding possible signals of non-equilibrium phenomena. All these modes yield continuum dileptons. However it is known that non-equilibrium dynamics can give rise to narrow peaks in spectral densities which have no relation to the equilibrium energy levels of the system [7]. This feature seems so generic that one wonders whether such a peak may not be seen in heavy-ion collisions. The moral I want to draw is that experiments should keep watch for phenomena which theories cannot yet deal with. Non-equilibrium statistical physics is a growing new branch of fundamental physics and heavy-ion experiments can make important contributions here.

To turn to concrete physics, I shall divide my talk into two major parts. The first will be concerned with continuum dileptons in various mass regions; the second with a few selected resonances. These are discussed in the next two sections. I shall emphasise the utility of lattice computations to guide phenomenology. The point is that the lattice is a non-perturbative tool to compute matrix elements in QCD which are usually obtained in models or perturbation theory. Such work started a year ago [8] and is being pursued further [9].

## 2. The Continuum

Continuum dileptons may be useful as a probe for thermal matter. All computations of the thermal signal to date have been performed in high temperature perturbation theory. Lattice computations give clear evidence for non-perturbative phenomena at temperatures close to  $T_c$ . It would, therefore, be interesting to obtain non-perturbative lattice estimates for the relevant QCD matrix elements at high temperature. This is now being done; the results will be available in the near future.

I shall speak of the high mass ( $M \gtrsim 5$  GeV), low mass ( $M \lesssim 1$  GeV) and the intermediate mass region. Roughly speaking, the intermediate mass region is bounded by the  $\rho$  and  $J/\psi$  resonances. I shall also speak of the region with  $M \gtrsim 10$  GeV as the very-high mass region. This is the region beyond the  $\Upsilon$  resonances.

### 2.1. Low mass continuum

In hadron-hadron collisions, the low-mass continuum seems to be understood in terms of several processes— Dalitz pairs, bremsstrahlung from pions *etc.* There have been quantitative attempts to extend this picture to heavy-ion collisions [10]. The low-mass dilepton spectrum may be strongly dependent on properties of thermalised hadronic matter, specially if the thermalisation time turns out to be close to this year's favourite number— a fraction of a fermi. A first attempt at such estimates now exists [11]. Such computations need, quite crucially, input on hadronic masses, widths and interaction strengths at finite temperatures. These can be obtained in lattice computations, and I shall summarise a recent computation [9] in the next section.

### 2.2. High mass continuum

Even if thermalisation times are short, the high mass continuum cross section consists of pre-equilibrium processes. The very high mass region is expected to consist essentially of Drell-Yan pairs at both the LHC and RHIC energies. At LHC, in the mass range between the  $\Upsilon$  and  $J/\psi$ , there could be substantial contribution from open bottom production.

This has yet to be estimated.

A state-of-the-art computation of rates for LHC and RHIC was presented in the Aachen Workshop in 1990 [12]. These were based on exponentiated  $\mathcal{O}(\alpha_s)$  cross sections computed in perturbative QCD [13]. Needless to say, these cross sections agree extremely well with data obtained in the range of energies  $19.4 \leq \sqrt{S} \leq 640$  GeV [14]. There have been two advances since the last estimates were made. One is theoretical—the full  $\mathcal{O}(\alpha_s^2)$  Drell-Yan cross section has now been computed [15]. In the high mass region these do not affect the old estimates. The second advance is experimental—measurements of structure functions in the range  $x \leq 10^{-3}$  have now been performed [16]. These have possible effect on estimates of cross sections at LHC energies; and must be taken into account once the data from HERA has been analysed.

The main kinematic features of the Drell-Yan cross section are the following. With increasing  $\sqrt{S}$ , the rapidity distribution of Drell-Yan pairs develops a plateau. At RHIC energies this is 3 units wide; at LHC energies the width increases to about 5 units. With increasing  $\sqrt{S}$ , at fixed  $M$ , the increase in the  $p_T$ -integrated cross section comes from the growth of the perturbative tail in the  $p_T$ -distribution. A consequence of this is a roughly linear growth of  $\langle p_T^2 \rangle$  with  $S$  which occurs for  $\sqrt{S} \gtrsim 50$ –100 GeV. Detailed predictions are given in [12].

It should be remembered that there are no mass scales involved in the QCD predictions apart from  $\Lambda_{QCD}$ . Thus absolute normalisations of cross sections,  $\langle p_T^2 \rangle$ , *etc*, and their dependence on  $\sqrt{S}$  are predictions. Approximate Monte-Carlo schemes [2], on the other hand, contain various mass parameters in momentum cutoffs. Thus absolute normalisations and other such dimensional quantities are fitted at each  $\sqrt{S}$  separately. As a result of this, it is necessary that these Monte Carlo generators be compared with a proper Drell-Yan estimate and data at all relevant values of  $\sqrt{S}$ .

### 2.3. Intermediate mass continuum

The intermediate region of the dilepton continuum comes from a complex mixture of sources. This is probably the most poorly understood part of the continuum spectrum. It is also the most important region for the continuum thermal dilepton signal. If the initial temperature is around 250 MeV, then it turns out that the thermal signal vanishes below the extrapolated Drell-Yan cross section at  $M \approx 2$ –2.5 GeV. If the initial temperature turns out to be about 1 GeV, then this signal may be visible above the same background even for  $M \approx 5$  GeV [17].

The extrapolation of Drell-Yan cross sections into this region suffers from two main ambiguities. The strongest source of uncertainty is in the parton luminosities at small  $x$ . At LHC, the range of masses of interest corresponds to  $x \approx 5 \times 10^{-4}$ . New physics may come into play in this region of kinematics. Structure function measurements now being done at HERA will be crucial for a better understanding of this region. A second uncertainty is in the importance of higher order resummed perturbative corrections. The new results mentioned above show that these are under control. I estimate an uncertainty of a factor of three when extrapolating Drell-Yan results to the intermediate mass range at RHIC and LHC energies. The thermal signal turns out to have a much steeper slope than the Drell-Yan continuum. Hence this large uncertainty still yields a small error (less than 0.5 GeV) in the cutoff mass below which the thermal signal dominates over this

background.

It should be remembered that the Drell-Yan process is only one of the many backgrounds in the dilepton channel in the intermediate mass region. At the higher end of this region decays of heavy-flavour quarks give rise to a large dilepton rate. Such a contribution had been pointed out by Shor long back. A minijet computation [19] for the process

$$A + B \rightarrow \text{jets} \rightarrow c(b) \rightarrow \text{leptons}, \quad (1)$$

shows that one should expect a large number of single leptons per event. These combine into a large dilepton background. This is relatively innocuous, since the rate for unlike sign is the same as for like sign pairs, and thus can be subtracted. A detailed Monte Carlo study is reportedly in progress [20]. More problematic is the background from the cascade decay of bottom into strange with unlike sign pairs. This background also needs to be computed.

At the lower end of the intermediate mass range the situation is even more complicated. The processes which contribute in heavy-ion collisions have probably not been completely enumerated yet. NA36 has some new data which they will discuss in this meeting [21].

#### 2.4. The deconfined phase

The continuum dimuon cross section in the deconfined phase is the signal for which the processes discussed in the previous subsections are the background. It is customary to compute this cross section in high-temperature perturbation theory. The lattice can furnish cross checks on this procedure.

In recent years several studies of lattice QCD [22,8] have furnished evidence that the high temperature phase really consists of deconfined quarks. Thus the primary condition for perturbation theory seems to be validated—the degrees of freedom are correctly identified.

However, there are indications that these quarks, under certain circumstances, have fairly strong self-interactions. A study [8] has clarified this situation. For mass scales below the Debye screening mass, one could write an effective theory for the quarks in the form

$$S_{eff} = \int d^4x \left[ \bar{\psi}(\gamma_\mu \partial_\mu + m)\psi + \sum_\Gamma g_\Gamma (\bar{\psi}\Gamma\psi)^2 + \dots \right], \quad (2)$$

where  $\Gamma$  denotes a direct product of spin and flavour matrices, and the sum is over the whole set of such products. The ellipsis denote neglected terms of higher mass dimension. From lattice measurements it has been found [8] that, although the effective couplings  $g$  in the scalar and pseudo-scalar channels are large, those in the vector and pseudo-vector channels are rather small already at temperatures close to  $T_c$ . Thus, this observation implies that perturbative computations of dilepton and photon production rates may be reliable quite close to the phase transition temperature. A similar computation in unquenched QCD is now in progress.

For  $T < 1.2T_c$ , however, perturbation theory does break down. This is reflected in the growth of all the effective couplings as one approaches  $T_c$  from above. It may be possible to use lattice measurements to obtain the matrix element relevant to photon or dilepton cross sections. Such studies are planned.

### 3. The Resonances

Heavy-quark resonances have been the subject of concerted study for the last five years. The situation is slowly being clarified; there is new and exciting data this year from the NA38 collaboration [23]. Lighter resonances have been studied in models for many years now. There is exciting news on these from recent lattice computations.

#### 3.1. Charmonium

Based on lattice studies of the static inter-quark potential, heavy-quarkonia have been suggested as a signal for screening. Screening sets in at the QCD phase transition and the screening length decreases with increasing  $T$ . Consequently, different resonances are suppressed to different extent under the same physical circumstances. This year's result from NA38 [23] shows a strong  $E_T$ -dependence to the relative suppression between the  $\psi'$  and the  $J/\psi$ . The data is compatible with estimates given in [24] as well as in [25].

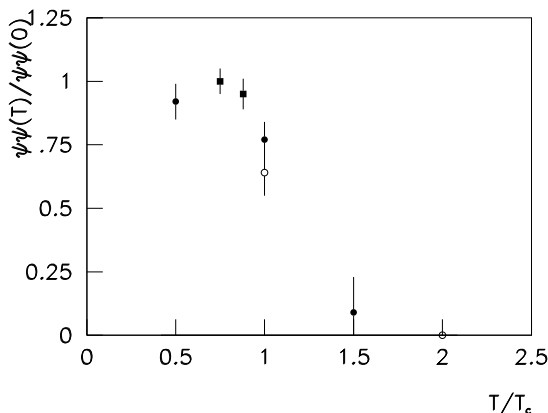


Figure 1. The temperature dependence of  $\langle\bar{\psi}\psi\rangle$ , for quenched simulations with  $N_\tau = 4$  (filled circles) and 8 (squares) and from a 4-flavour simulation with  $N_\tau = 8$  (open circles).

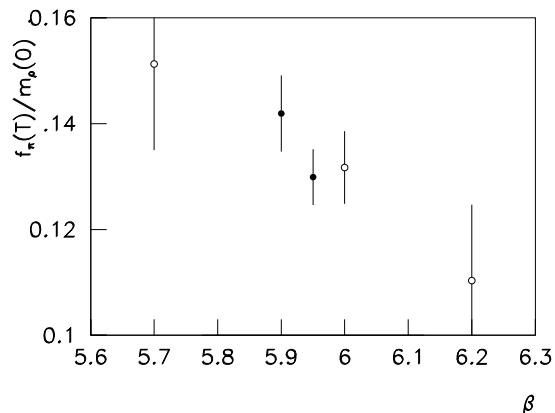


Figure 2. The temperature dependence of  $f_\pi$ . Data for  $T = 0$  (open circles) and at finite temperatures (filled circles)  $T \approx 0.75T_c$  ( $\beta = 5.9$ ) and  $T \approx 0.9T_c$  ( $\beta = 5.95$ ).

#### 3.2. The $\rho$ meson

Two recent studies of quenched lattice QCD have concentrated on hadronic properties for  $0 < T < T_c$ . One of these [8] was done on  $N_\tau = 4$  lattices on very large spatial volumes, extending to  $(8/T)^3$ , at  $0.5T_c$ . Work now in progress [9] extends these computations to  $N_\tau = 8$  on spatial volumes of  $(4/T)^3$  at  $0.75T_c$  and  $0.88T_c$ . In both these studies the values of the quark condensate,  $\langle\bar{\psi}\psi\rangle$ , pion decay constant,  $f_\pi$ , and the pion and  $\rho$  masses have been studied. The temperature dependence of these quantities is obtained by comparison with  $T = 0$  measurements at the same lattice spacing.

It is known that the quark condensate goes to zero with a discontinuity at  $T_c$  in both the quenched [8,9] and 4-flavour [26] theories. In Figure 1 we show the measured temperature dependence of  $\langle\bar{\psi}\psi(T)\rangle/\langle\bar{\psi}\psi(0)\rangle$  (the  $T = 0$  values are taken from [27]). Two features bear comment. First, note that the discontinuity at  $T_c$  is similar in the two cases. Second,  $\langle\bar{\psi}\psi\rangle$  seems to be relatively temperature independent up to  $T \approx 0.9T_c$ .

A non-vanishing quark condensate implies a vanishing pion mass in the chiral limit. The physical pion mass is obtained from the relation

$$m_\pi^2 = A_\pi m_q. \quad (3)$$

Here  $m_q$  is the quark mass. Measurements of  $A_\pi$  on the lattice, thus give information on the temperature dependence of the pion mass. Our measurements reveal no change in  $A_\pi$  compared to the values at  $T = 0$  for temperatures up to  $0.9T_c$  (see Figure 3a). Consequent to these two facts, the pion decay constant,  $f_\pi$ , shows no change with temperature upto  $T = 0.9T_c$ . This is explicitly shown in Figure 2, using the data of [9] and the  $T = 0$  data of [28]. In Figures 1 and 2, mass ratios have been used in order to remove most lattice effects.

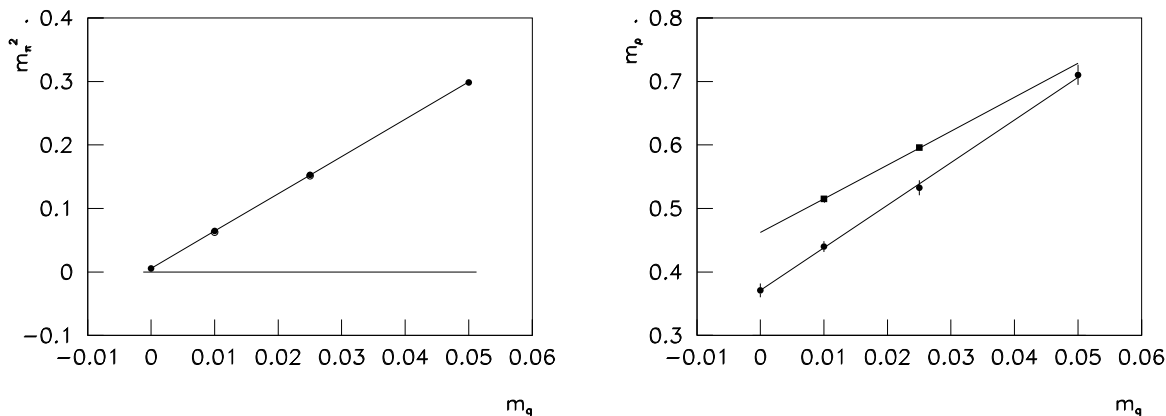


Figure 3. The dependence of (a)  $m_\pi^2$  and (b)  $m_\rho$  on  $m_q$  at  $T \approx 0.9T_c$  (circles) compared to data at  $T = 0$  (squares) at the same lattice spacing ( $\beta = 5.95$ ).

The value of  $m_\rho$ , on the other hand, seems to be quite strongly dependent on the temperature. Measurements show that there is very little shift in the vector meson masses at a temperature of  $0.75T_c$ . Within the errors of measurement, in fact, no shift is discernible. However, at  $0.9T_c$  there is a large temperature dependent shift, visible in Figure 3b. It is interesting that a large shift in the mass of the  $\rho$  meson occurs already at a temperature where the chiral sector of the theory sees no temperature effect.

It should be noted that most phenomenological models of the hadron spectrum and its temperature dependence emphasise chiral aspects of the theory. Thus the temperature dependence of the quark condensate is one of the primary objects of study. The vacuum of QCD, however, is characterised by many different condensates, some invisible to the chiral sector of the theory. In most phenomenological models, the temperature dependence of, say, the gluon condensate is a secondary quantity, often neglected. One interpretation of this lattice data is that some of these other condensates have strong temperature dependence. This would imply a dynamical role for the glue sector which is stronger than is usually assumed. Efforts to extract the temperature dependence of at least a few of these other condensates are now underway. If the influence of the glue sector is indeed so strong, then the use of an universal chiral theory at finite-temperatures to obtain information on vector and pseudo-vector mesons may not be justified.

The variation of the vector meson mass with the quark mass  $m_q$  is shown in Figure 3b at a temperature  $T \approx 0.9T_c$ . For comparison the corresponding data for  $T = 0$  at the same lattice spacing,  $\beta = 5.95$  [29], is also shown. It is seen that the magnitude of the thermal shift is dependent on  $m_q$ . Thus, the maximum effect is seen for the  $\rho$  meson, somewhat less for the  $\omega$  and  $\phi$ , and virtually none (at this temperature, at least) for any heavier meson. Of course, an accurate determination of the mass shift of a state heavier than the inverse lattice spacing is difficult.

It is interesting to speculate what the effect of differential shifts in the masses of the  $\rho$ ,  $\omega$  and  $\phi$  mesons would be on an experiment like NA38 which cannot resolve these separate peaks. An obvious effect would be to broaden this peak. Further phenomenology might be interesting.

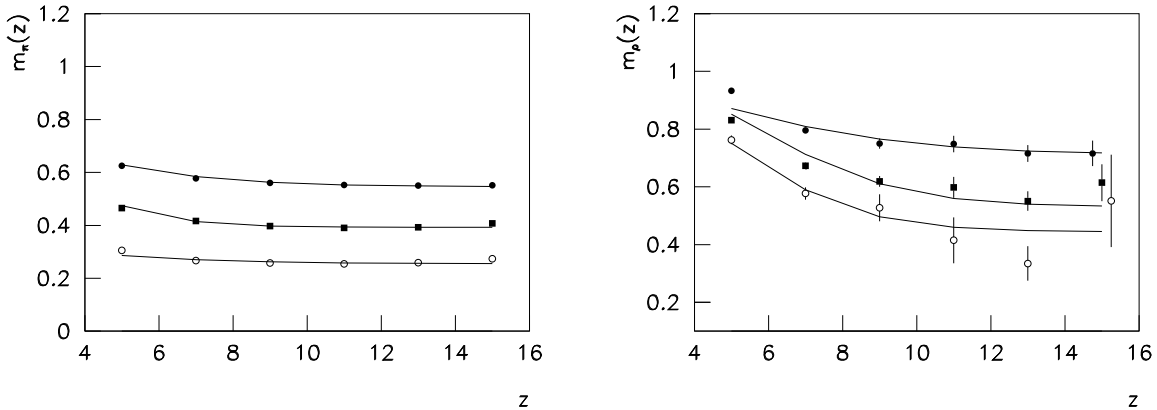


Figure 4. Local masses for the (a) pseudoscalar and (b) vector mesons at  $T \approx 0.9T_c$  ( $\beta = 5.95$ ) for  $m_q = 0.05$  (filled circles), 0.025 (squares) and 0.01 (open circles). The estimates and errors are obtained by jack-knife. The lines are explained in the text.

We conclude this section with some technical remarks. The masses reported here were extracted by global fits to vector and pseudoscalar correlation functions constructed from local sources. The well-known oscillatory behaviour in the vector channel was suppressed by the usual stratagem of defining a correlation function on even sites

$$G(2z) = \frac{1}{2}[G(2z-1) + 2G(2z) + G(2z+1)]. \quad (4)$$

Local masses were extracted assuming that this correlation function can be described by one mass, *i.e.*, by a single hyperbolic cosine. The global fits were made to a two-mass functional form by minimising a  $\chi^2$  functional which took into account the covariance of the measurements at different separations. An useful cross check is to use the fitted function to then extract ‘local masses’ to compare with the direct measurement. Such a comparison then checks the validity of the global fits. Example are given in Figure 4.

**Acknowledgements:** I would like to thank K. Eskola, R. Gavai, S. Gavin, A. Irbäck, F. Karsch, B. Petersson, V. Ruuskanen, H. Satz, K. Sridhar and R. Vogt for the discussions and/or collaborations, the results of which are reflected in this talk.



## REFERENCES

1. P. V. Ruuskanen, *Nucl. Phys. A* 544 (1992) 169c;  
J. I. Kapusta, these proceedings.
2. K. Kinder-Geiger, these proceedings.
3. M. Gyulassy, these proceedings.
4. E. Shuryak and L. Xiong, *Phys. Rev. Lett.* 70 (1993) 2241.
5. P. Huet *et al.*, preprint SLAC-PUB-5943, 1992; see also the talk by K. Kajantie in these proceedings.
6. G. Lana and B. Svetitsky, *Phys. Lett., B* 285 (1992) 251.
7. Sourendu Gupta, preprint HLRZ 22/93.
8. S. Gupta, *Phys. Lett. B* 288 (1992) 171.
9. G. Boyd, S. Gupta, F. Karsch, E. Laermann and B. Petersson, work in progress.
10. J. Cleymans, K. Redlich and H. Satz, *Z. Phys. C* 52 (1991) 517.
11. F. Karsch, K. Redlich and H. Turko, preprint HLRZ 19/93.
12. Sourendu Gupta, in *Proceedings of the ECFA-LHC Aachen Workshop*, eds G. Jarlskog and D. Rein, Vol II (1990) 1174.
13. G. Altarelli, R. K. Ellis, M. Greco and G. Martinelli, *Nucl. Phys. B* 246 (1984) 12.
14. A. G. Clark *et al.*, *Nucl. Phys. B* 142 (1978) 29;  
C. Kourkoumelis *et al.*, *Phys. Lett.* 91 B (1980) 475;  
A. S. Ito *et al.*, *Phys. Rev. D* 23 (1981) 604;  
J. Badier *et al.*, *Z. Phys. C* 26 (1985) 489;  
B. Betev *et al.*, *Z. Phys. C* 28 (1985) 9;  
C. Albajar *et al.*, *Phys. Lett. B* 209 (1988) 397;  
C. N. Brown *et al.*, *Phys. Rev. Lett.* 63 (1989) 2637.
15. R. Hamberg, W. L. van Neerven and T. Matsuura, *Nucl. Phys. B* 359 (1991) 343.
16. L. Jönsson, these proceedings.
17. J. I. Kapusta, L. McLerran and D. K. Srivastava, *Phys. Lett. B* 283 (1992) 145.
18. A. Shor, *Phys. Lett. B* 233 (1989) 231.
19. Sourendu Gupta, *Phys. Lett. B* 248 (1990) 453.
20. K. Eskola and X.-N. Wang, these proceedings.
21. NA36 collaboration, these proceedings.
22. K. D. Born *et al.*, *Phys. Rev. Lett.* 67 (1991) 302;  
G. Boyd, Sourendu Gupta and F. Karsch, *Nucl. Phys. B* 385 (1992) 481;  
G. Boyd, Sourendu Gupta, F. Karsch and E. Laermann, preprint HLRZ 54/93; reported by G. Boyd in these proceedings.
23. NA38 collaboration, these proceedings.
24. S. Gupta and H. Satz, *Phys. Lett. B* 283 (1992) 439.
25. S. Gavin, these proceedings.
26. R. V. Gavai *et al.*, *Phys. Lett. B* 241 (1990) 567.
27. G. Salinas and A. Vladikas, *Phys. Lett. B* 249 (1990) 119.
28. R. Gupta *et al.*, *Phys. Rev. D* 43 (1991) 2003.
29. K. M. Bitar *et al.*, *Nucl. Phys. B (Proc. Suppl.)* 20 (1991) 362.